

# Near to Far-Field Plane-Polar Transformation from Probe Positioning Error Affected Data

F. D'Agostino, F. Ferrara, C. Gennarelli, R. Guerriero, and M. Migliozi

Department of Industrial Engineering  
University of Salerno, via Giovanni Paolo II, 132 - 84084 Fisciano, Italy  
fdagostino@unisa.it, flferrara@unisa.it, cgennarelli@unisa.it, rguerriero@unisa.it, mmigliozi@unisa.it

**Abstract** — In this article, two efficient approaches for the correction of known positioning errors of the measurement probe in a plane-polar near to far-field (NTFF) transformation, requiring a minimum number of NF data in the case of quasi-planar antennas, are presented and experimentally assessed. Such a NTFF transformation benefits from a non-redundant sampling representation of the voltage detected by the probe got by modeling an antenna with a quasi-planar geometry through a double bowl, a surface consisting of two circular bowls with the same aperture radius, but with lateral bends which may differ to better fit the antenna shape. The uniform samples, i.e., those at the points set by the representation, are accurately retrieved from the collected not regularly distributed ones either by applying a singular value decomposition based approach or an iterative scheme. Then, the input NF data necessary for the classical plane-rectangular NTFF transformation are evaluated from the so retrieved non-redundant uniform samples through a 2-D optimal sampling interpolation formula.

**Index Terms** — Antenna measurements, non-redundant representations of electromagnetic fields, plane-polar near to far-field transformation, positioning errors correction.

## I. INTRODUCTION

The near to far-field (NTFF) transformation techniques [1-5] are well-assessed and commonly employed tools for the precise evaluation of the radiation pattern of antennas having large dimensions in terms of wavelengths from NF measurements made in an anechoic chamber, which suitably reproduces the free-space propagation conditions by suppressing almost completely the reflections from its walls. Among these transformations, the traditional plane-rectangular one [6, 7] is especially suitable when dealing with high gain antennas which radiate pencil beam patterns. For these antennas, an even more convenient transformation is the one using the plane-polar scan [8-14], which offers the following advantages compared to the plane-rectangular one: i) a simpler mechanical realization, since it can be achieved via a linear movement

of the measuring probe and a rotary motion of the antenna under test (AUT); ii) a larger scanning zone for the same dimensions of the anechoic chamber; iii) a more precise measurement of the radiation patterns of gravitationally sensitive spaceborne AUTs when the scanning is accomplished in a horizontal plane. In order to make the number of the required NF data and corresponding measurement time remarkably smaller than those in [8-10], the non-redundant sampling representations of electromagnetic (EM) fields [15] have been suitably applied in [11, 12] to the voltage detected by a non-directive probe, thus developing 2-D optimal sampling interpolation (OSI) formulas, which allow one to accurately recover the NF data necessary for the traditional plane-rectangular NTFF transformation [6, 7] from a minimum number of plane-polar ones. In particular, the AUTs have been considered as contained inside a surface formed by two circular bowls having the same aperture and possibly different lateral surfaces (double bowl) in [11], whereas an oblate ellipsoidal surface has been employed to model them in [12]. The experimental assessments of the non-redundant plane-polar NTFF transformations [11] and [12] have been then provided in [13] and [14], respectively.

It must be noticed that, as a consequence of a not accurate control of the positioners and/or of their limited resolution, it could not be possible to acquire the NF data at the points prescribed by the non-redundant sampling representation, even if their actual positions can be precisely revealed through laser interferometric techniques. Hence, the fulfillment of an efficient and robust procedure, that enables a possibly precise retrieval of the NF data to be employed in the traditional plane-rectangular NTFF transformation from the positioning errors affected (non-uniform) plane-polar ones, appears of fundamental importance. To this purpose, a procedure relying on the conjugate gradient iterative technique and adopting the fast Fourier transform (FFT) for non-equispaced data [16] has been applied for correcting known position errors in the traditional NTFF transformations adopting the planar [17] and spherical [18] scans. However, this procedure is not appropriate for the non-redundant plane-polar NTFF

transformations [11, 12], wherein efficient OSI expansions are applied to precisely evaluate the NF data necessary for the traditional plane-rectangular NTF transformation from the collected non-redundant plane-polar samples. As underlined in [19, 20], where a more complete discussion on the non-uniform sampling can be found, the formulas which allow the direct retrieval of the needed data from the non-uniform samples are not stable and easy to use, and are valid only for specific samples grids. A convenient and feasible policy [19] is to retrieve the regularly distributed (uniform) samples from the non-uniform ones and then reconstruct the required NF data by using a precise and stable OSI formula. To reach this goal, two distinct procedures have been proposed. The former adopts an iterative technique, converging only if it is possible to set up a bijective relation linking every uniform sampling point to the nearest non-uniform one, and has been used to reconstruct the uniform samples in a plane-rectangular grid [19]. The latter utilizes the singular value decomposition (SVD) method, does not show the above shortcoming, allows one to benefit from the redundancy of the data to increase the algorithm robustness as regards errors corrupting them, and has been exploited to develop non-redundant NTF transformations from positioning errors affected samples adopting the plane-polar [21], bi-polar [22], and cylindrical [23] scans. In any case, the SVD based approach can be gainfully employed if the starting 2-D problem of the regularly spaced samples retrieval can be subdivided in two independent 1-D problems; if this is not the case, the dimensions of the related matrices remarkably increase, so that a massive computing effort is needed. Both the procedures have been compared through simulations and experimentally assessed with reference to the cylindrical [24] and spherical [20, 25-27] scans, whereas their effectiveness in the plane-polar NTF transformation when using an oblate ellipsoidal AUT modeling has been experimentally demonstrated in [28].

The aim of the article is to suitably extend the application of these techniques to the correction of known positioning errors in the non-redundant NTF transformation with plane-polar scan [11, 13], which adopts a double bowl to shape a quasi-planar antenna (Fig. 1), and to experimentally demonstrate their effectiveness through a measurement campaign executed at the Antenna Characterization Lab of the UNIVERSITY of SALerno (UNISA).

## II. NON-REDUNDANT REPRESENTATION OF THE PROBE VOLTAGE ON A PLANE FROM NON-UNIFORM SAMPLES

### A. Uniform samples representation

The non-redundant sampling representation of the voltage detected by a not directive probe, which scans a plane at distance  $d$  from the aperture of a quasi-planar AUT via a plane-polar NF system, and the corresponding OSI expansion are briefly recalled in this subsection for the

case wherein a double bowl model is adopted [11, 13]. The spherical coordinate system  $(r, \vartheta, \varphi)$  is used for denoting the observation point, while the plane-polar coordinates  $(\rho, \varphi)$  are also used to identify a point  $P$  on the plane (Fig. 1). A double bowl is a surface  $\Sigma$  obtained by joining together two circular bowls having the same aperture radius  $a$ , but possibly not equal bending radii  $h$  and  $h'$  of the upper and lower arcs to allow a better fitting of the actual antenna geometry (see Figs. 1 and 2). As mentioned in the Introduction, the non-redundant sampling representations [15] can be advantageously exploited to represent the voltage detected by a not directive probe, because its spatial bandwidth practically coincides with that of the antenna radiated field [29]. According to these representations, an optimal parameter  $\eta$  must be adopted for describing any of the curves  $\Gamma$  (diameters and rings) representing the plane in a plane-polar frame, and a suitable phase factor  $e^{-j\psi(\eta)}$  has to be singled out from the voltage  $V_\varphi$  or  $V_\rho$  detected by the scanning probe in its two orientations (probe/rotated probe). The so introduced “reduced voltage”:

$$\tilde{V}(\eta) = V(\eta)e^{j\psi(\eta)}, \quad (1)$$

is spatially almost bandlimited and not strictly bandlimited, so that an error arises when it is approximated by means of a bandlimited function. In any case, this bandlimitation error can be made reasonably small as the band-width is larger than a critical value  $W_\eta$  [15] and effectively reduced by considering an increased bandwidth  $\chi'W_\eta$ ,  $\chi'$  being an enlargement bandwidth factor a bit larger than one for AUTs having electrical large sizes [15].

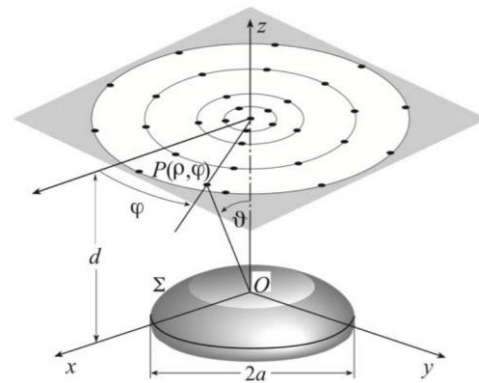


Fig. 1. Plane-polar scanning for a quasi-planar antenna.

If  $\Gamma$  is a diameter, by choosing  $W_\eta = \beta\ell'/2\pi$  it results [11, 13]:

$$\psi = (\beta/2)[R_1 + R_2 + s'_1 - s'_2], \quad (2)$$

$$\eta = (\pi/\ell')[R_1 - R_2 + s'_1 + s'_2], \quad (3)$$

wherein  $\ell' = 4a + (h + h')(\pi - 2)$  is the length of the

intersection curve  $C'$  between the meridian plane passing through the observation point  $P$  and the double bowl  $\Sigma$ ,  $\beta$  is the wavenumber,  $R_{1,2}$  are the distances from  $P$  to the two tangency points  $P_{1,2}$  between  $C'$  and the cone with the vertex at  $P$ , and  $s'_{1,2}$  their curvilinear abscissas (see Fig. 2). The values of  $s'_{1,2}$  and  $R_{1,2}$  change depending on the radial distance  $\rho(\eta)$ . It can be easily verified that, when  $\rho < a$ , the tangency points  $P_{1,2}$  are situated on the upper bowl, whereas, when  $\rho > a$ ,  $P_1$  is still on the upper bowl and  $P_2$  is located on the lower one. The corresponding expressions of  $s'_{1,2}$  and  $R_{1,2}$  can be evaluated in a straightforward manner and are explicitly reported in [11, 13].

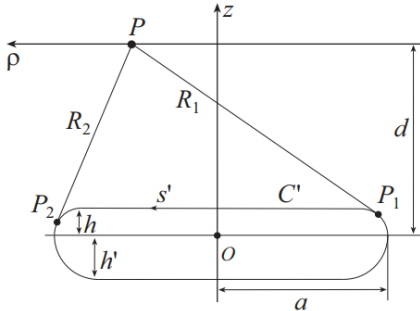


Fig. 2. Relevant to the double bowl modeling.

If  $\Gamma$  is a ring,  $\psi$  results to be constant and the angle  $\varphi$  can be conveniently used as optimal parameter. The corresponding bandwidth  $W_\varphi$  is [11, 13]:

$$W_\varphi = \frac{\beta}{2} \max_{z'} (R^+ - R^-) = \frac{\beta}{2} \max_{z'} \left( \sqrt{(\rho + \rho'(z'))^2 + (d - z')^2} - \sqrt{(\rho - \rho'(z'))^2 + (d - z')^2} \right), \quad (4)$$

where  $\rho'(z')$  is the equation of the surface  $\Sigma$  and  $R^+$ ,  $R^-$  are the maximum and minimum distances from  $\Gamma$  to the circumference of  $\Sigma$  at  $z'$ . The explicit evaluation of such a maximum is detailed in [11, 13].

At each point  $P(\rho, \varphi)$  on the plane, the voltage can be efficiently evaluated through the following OSI expansion [11, 13]:

$$V(\eta(\rho), \varphi) = e^{-j\psi(\eta)} \sum_{n=n_0-q+1}^{n_0+q} \tilde{V}(\eta_n, \varphi) A(\eta, \eta_n, \bar{\eta}, N, N''), \quad (5)$$

wherein  $n_0 = n_0(\eta) = \text{Int}(\eta/\Delta\eta)$ ,  $2q$  is the number of the considered nearest intermediate samples  $\tilde{V}(\eta_n, \varphi)$ , namely, the reduced voltages at the intersections between the diameter through  $P$  and the sampling rings,

$$A(\eta, \eta_n, \bar{\eta}, N, N'') = \Omega_N(\eta - \eta_n, \bar{\eta}) D_{N''}(\eta - \eta_n), \quad (6)$$

is the OSI interpolation function,

$$\eta_n = n\Delta\eta = 2\pi n/(2N''+1); \quad N'' = \text{Int}(\chi N') + 1, \quad (7)$$

$$N' = \text{Int}(\chi' W_\eta) + 1; \quad N = N'' - N'; \quad \bar{\eta} = q\Delta\bar{\eta}. \quad (8)$$

$\text{Int}(x)$  denotes the greatest integer less than or equal to  $x$ , and  $\chi$  is the oversampling factor needed to control the truncation error [15]. In (6),

$$\Omega_N(\eta, \bar{\eta}) = \frac{T_N \left[ \frac{2\cos^2(\eta/2) / \cos^2(\bar{\eta}/2) - 1}{2/\cos^2(\bar{\eta}/2) - 1} \right]}{T_N \left[ \frac{2/\cos^2(\bar{\eta}/2) - 1}{2/\cos^2(\bar{\eta}/2) - 1} \right]}, \quad (9)$$

and

$$D_{N''}(\eta) = \frac{\sin[(2N''+1)\eta/2]}{(2N''+1)\sin(\eta/2)}, \quad (10)$$

are the Tschebyscheff and Dirichlet sampling functions [15],  $T_N(\eta)$  being the Tschebyscheff polynomial of degree  $N$ .

The intermediate samples can be determined by interpolating the samples on the rings through the OSI formula [11, 13]:

$$\tilde{V}(\eta_n, \varphi) = \sum_{m=m_0-p+1}^{m_0+p} \tilde{V}(\eta_m, \varphi_{m,n}) A(\varphi, \varphi_{m,n}, \bar{\varphi}_n, M_n, M_n''), \quad (11)$$

wherein  $m_0 = m_0(\varphi) = \text{Int}(\varphi/\Delta\varphi_n)$ ,  $2p$  is the number of the considered nearest samples on the ring specified by  $\eta_n$ , and

$$\varphi_{m,n} = m\Delta\varphi_n = 2\pi m/(2M_n''+1); \quad M_n'' = \text{Int}(\chi M_n') + 1, \quad (12)$$

$$M_n' = \text{Int}[\chi^* W_\varphi(\eta_n)] + 1; \quad M_n = M_n'' - M_n', \quad (13)$$

$$\chi^* = 1 + (\chi' - 1) [\sin \mathcal{G}(\eta_n)]^{2/3}; \quad \bar{\varphi}_n = p\Delta\varphi_n. \quad (14)$$

The 2-D OSI expansion, which allows the accurate reconstruction of  $V_\varphi$  and  $V_\rho$  at any point in the measurement circle, is easily attained by properly matching the 1-D expansions (5) and (11). It can be exploited to reconstruct in a fast and accurate way these voltages at the points necessary for the plane-rectangular NTF transformation [6, 7]. However, the probe corrected formulas in [7] (whose expressions in the here used reference system are shown in [13, 30]) are valid only when the probe keeps its orientation with respect to the AUT and this requires its co-rotation with it. In order to avoid this co-rotation, a probe with a far field having a first-order  $\varphi$ -dependence must be utilized. In this case, the voltages  $V_V$  and  $V_H$  (acquired with co-rotation by the probe and rotated probe) are related to  $V_\varphi$  and  $V_\rho$  by:

$$V_V = V_\varphi \cos \varphi - V_\rho \sin \varphi; \quad V_H = V_\varphi \sin \varphi + V_\rho \cos \varphi, \quad (15)$$

thus enabling a ‘‘software co-rotation’’. To this end, an open-ended rectangular waveguide can be conveniently used as scanning probe. In fact, the far field radiated in the forward hemisphere by it, when excited by a  $\text{TE}_{10}$  mode, has in a practically good approximation a first-order azimuthal dependence [31].

## B. Uniform samples recovery

In this subsection, two effective techniques for

correcting NF data affected by known positioning errors in the described non-redundant plane-polar NTF transformation are presented by pointing out their benefits and shortcomings.

The former technique relies on the SVD method. In such a case, it is supposed that, save for the sample at  $\rho=0$ , all the other are not regularly spaced on rings not uniformly distributed on the scanning plane. This hypothesis is indeed realistic if the plane-polar NF data are collected by performing the scan along the rings as needed to benefit from the reduction of the number of NF data on the most inner rings, obtainable when exploiting the previous non-redundant sampling representation. In this case, the problem of the uniform samples retrieval can be subdivided in two independent 1-D problems.

The uniform  $2M_k''+1$  samples on a non-uniform ring at  $\rho(\xi_k)$  are recovered as follows. By considering a set of  $J_k \geq 2M_k''+1$  non-uniform sampling points  $(\xi_k, \phi_j)$  on this ring and expressing the corresponding reduced voltages  $\tilde{V}(\xi_k, \phi_j)$  in terms of the unknown ones at the uniform sampling points  $(\xi_k, \varphi_{m,k})$ , the linear system:

$$\underline{\underline{C}} \underline{X} = \underline{B}, \quad (16)$$

is attained, wherein  $\underline{B}$  is the known non-uniform samples vector,  $\underline{X}$  is that of the unknown uniform ones  $\tilde{V}(\xi_k, \varphi_{m,k})$ , and  $\underline{\underline{C}}$  is a  $J_k \times (2M_k''+1)$  sized matrix. The element of the matrix  $\underline{\underline{C}}$  are:

$$c_{jm} = A(\phi_j, \varphi_{m,k}, \bar{\varphi}_k, M_k, M_k''), \quad (17)$$

wherein  $\varphi_{m,k} = m\Delta\varphi_k = 2m\pi/(2M_k''+1)$  and  $\bar{\varphi}_k = p\Delta\varphi_k$ . It is worthy to observe that, for a given row  $j$ , the elements  $c_{jm}$  are zero when the index  $m$  is outside the range  $[m_0(\phi_j) - p + 1, m_0(\phi_j) + p]$ . The SVD is then applied to get the best least square approximated solution of (16). After such a step, the intermediate samples  $\tilde{V}(\xi_k, \varphi)$  in correspondence of the intersections between the non-uniform rings and the diameter passing through  $P$  are recovered via the OSI expansion (11), wherein the samples  $\tilde{V}(\xi_k, \varphi_{m,k})$  take the place of the  $\tilde{V}(\eta_n, \varphi_{m,n})$  ones. Since these intermediate samples are not regularly distributed, the voltage at  $P$  can be reconstructed by first recovering the regularly distributed intermediate samples  $\tilde{V}(\eta_n, \varphi)$  again by applying the SVD method and subsequently interpolating them through the OSI expansion (5).

It must be stressed that either the distances from each non-uniform ring to the corresponding uniform one and the ones between the non-uniform sampling points and the associated uniform ones on the non-uniform rings have been supposed less than one half of the related uniform spacing for avoiding a severe ill-conditioning of the correlated linear system. In addition, in order to minimize the computational effort, an equal number  $N_\varphi$  of uniform samples, coincident with that corresponding to the outer uniform ring, has been reconstructed on each non-uniform

ring. In this way, the samples are aligned along the diameters and, therefore, the number of systems to be solved is minimum.

At last,  $V_\varphi$  and  $V_\rho$  at the points necessary for the traditional plane-rectangular NTF transformation [6, 7] are efficiently reconstructed via the OSI expansions (5) and (11), this latter appropriately adapted to account for the redundancy in  $\varphi$ .

The latter technique adopts an iterative scheme, converging only if it is possible to set up a bijective relation linking each uniform sampling point to the nearest non-uniform one. In this case, the number  $Q$  of the non-uniform samples must be the same as that of the uniform ones. Moreover, it is now supposed that, except the sample at  $\rho=0$ , all the other are not regularly spaced on the scanning plane, do no longer lie on rings, but must satisfy the above bijective correspondence. By applying the OSI expansions (5) and (11), it is possible to express the reduced voltages at each non-uniform sampling point  $(\xi_k, \phi_{j,k})$  in terms of those unknown at the nearest uniform sampling points  $(\eta_n, \varphi_{m,n})$ , thus getting the linear system:

$$\tilde{V}(\xi_k, \phi_{j,k}) = \sum_{n=n_0-q+1}^{n_0+q} \left\{ A(\xi_k, \eta_n, \bar{\eta}, N, N'') \cdot \sum_{m=m_0-p+1}^{m_0+p} \tilde{V}(\eta_n, \varphi_{m,n}) A(\phi_{j,k}, \varphi_{m,n}, \bar{\varphi}_n, M_n, M_n'') \right\}, \quad (18)$$

which can be again recast in the matrix form (16), wherein  $\underline{\underline{C}}$  is now a  $Q \times Q$  sized matrix. Such a linear system could be solved via the SVD method, but a huge computational effort would be required. On the contrary, it can be efficiently solved by applying an iterative algorithm, which is derived as described in the following. In the first step, the matrix  $\underline{\underline{C}}$  is subdivided in its diagonal part  $\underline{\underline{C}}_D$  and non-diagonal part  $\underline{\underline{\Delta}}$ , subsequently, both the sides of the relation  $\underline{\underline{C}} \underline{X} = \underline{B}$  are multiplied by  $\underline{\underline{C}}_D^{-1}$ , and, finally, its terms are rearranged thus obtaining the iterative scheme:

$$\underline{X}^{(v)} = \underline{\underline{C}}_D^{-1} \underline{B} - \underline{\underline{C}}_D^{-1} \underline{\underline{\Delta}} \underline{X}^{(v-1)} = \underline{X}^{(0)} - \underline{\underline{C}}_D^{-1} \underline{\underline{\Delta}} \underline{X}^{(v-1)}, \quad (19)$$

with  $\underline{X}^{(v)}$  being the uniform samples vector obtained at the  $v$ th iteration.

To guarantee the convergence of such an iterative scheme, it is necessary but not sufficient, as stressed in [19], that the amplitude of every element belonging to the main diagonal of the matrix  $\underline{\underline{C}}$  be different from zero and larger than the amplitudes of the other elements which lie on the same column or row. It can be easily verified that the assumed hypothesis of bijective relation between each uniform sampling point and the "nearest" non-uniform one ensures the fulfillment of these conditions. By putting relation (19) in explicit form, it results:

$$\begin{aligned} \tilde{V}^{(v)}(\eta_m, \varphi_{m,n}) &= \\ &= \frac{1}{A(\xi_n, \eta_n, \bar{\eta}, N, N'')A(\phi_{m,n}, \varphi_{m,n}, \bar{\varphi}_n, M_n, M_n'')} \cdot \\ &\left\{ \tilde{V}(\xi_n, \phi_{m,n}) - \sum_{s=s_0-q+1}^{s_0+q} \sum_{\substack{i=i_0-p+1 \\ (s \neq n) \wedge (i \neq m)}}^{i_0+p} A(\xi_n, \eta_s, \bar{\eta}, N, N'') \cdot \right. \\ &\left. \cdot A(\phi_{m,n}, \varphi_{i,s}, \bar{\varphi}_s, M_s, M_s'') \tilde{V}^{(v-1)}(\eta_s, \varphi_{i,s}) \right\}, \quad (20) \end{aligned}$$

where

$$s_0 = \begin{cases} n & \text{if } \xi_n \geq \eta_n \\ n-1 & \text{if } \xi_n < \eta_n \end{cases}; \quad i_0 = \begin{cases} m & \text{if } \phi_{m,n} \geq \varphi_{m,s} \\ m-1 & \text{if } \phi_{m,n} < \varphi_{m,s} \end{cases}. \quad (21)$$

### III. EXPERIMENTAL ASSESSMENT

Some results of laboratory tests performed in the anechoic chamber of the UNISA Antenna Characterization Lab are shown in this section to give the experimental assessment of the two described techniques for compensating the probe positioning errors. The chamber is  $8\text{m} \times 5\text{m} \times 4\text{m}$  sized and is provided with a plane-polar NF scanning system, besides the cylindrical and spherical ones. The pyramidal absorbers, covering the chamber walls, assure a reflection level lesser than  $-40$  dB. A vector network analyzer is utilized to accomplish the measurements of the amplitude and phase of the voltage detected by the adopted probe, an open-ended WR-90 rectangular waveguide. The plane-polar scan is attained by attaching the probe to a linear vertical positioner and putting the AUT on a rotating table, whose rotary axis is normal to the linear positioner. A further rotating table has been recently integrated in the NF scanning system. It has been placed between the linear positioner and the probe and allows to perform a plane-polar scan, wherein the probe axes keep their orientation with respect to AUT ones (hardware co-rotation), as well as to measure the NF data which would be collected by a plane-rectangular NF facility. The considered AUT is a dual pyramidal horn antenna with vertical polarization, positioned on the plane  $z=0$  of the adopted reference system (Fig. 1) and working at 10 GHz. The horns aperture has sizes  $8.9\text{cm} \times 6.8\text{cm}$  and the distance between the apertures centers is 26.5 cm. This AUT has been modeled by a double bowl with  $a = 18.0$  cm and  $h = h' = 3.0$  cm. The non-uniform, as well as the uniform, NF plane-polar samples considered in the shown results have been acquired on a circle having radius 110 cm on a plane at distance  $d = 16.5$  cm from the AUT.

In Figs. 3 and 4, the E- and H-planes FF patterns reconstructed from the non-redundant plane-polar NF samples acquired with the hardware co-rotation are compared with those got from the plane-rectangular NF data directly measured, at the sample spacing of  $0.45\lambda$ , on the  $140\text{cm} \times 140\text{cm}$  inscribed square. As can be seen, a very good agreement is found in both the

planes. The corresponding recoveries, obtained from the non-redundant plane-polar NF samples acquired when using the software co-rotation, are shown in Figs. 5 and 6. In such a case, especially in the H-plane, a less accurate reconstruction results. This is due to the fact that the far field radiated by an open-ended rectangular waveguide excited by a  $\text{TE}_{10}$  mode has only approximately a first-order azimuthal dependence [31].

Let us now turn to the case of irregularly spaced samples. The first set of figures (Figs. 7 - 11) refers to the case of not uniformly distributed sampling points which lie on rings. The NF data have been acquired in such a way that the distances from every non-uniform ring to the corresponding uniform one, and those between the non-uniform sampling points and the related uniform ones on the rings are random variables with uniform distributions in  $(-\Delta\eta/2, \Delta\eta/2)$  and  $(-\Delta\varphi_k/2, \Delta\varphi_k/2)$ , respectively.

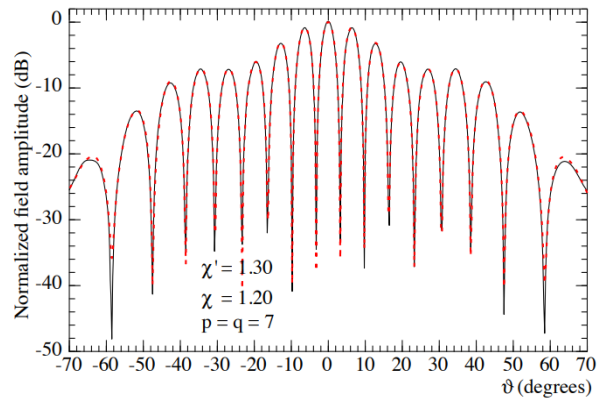


Fig. 3. E-plane pattern. — reconstructed from plane-rectangular NF data. - - - reconstructed from the non-redundant plane-polar NF samples with hardware co-rotation.

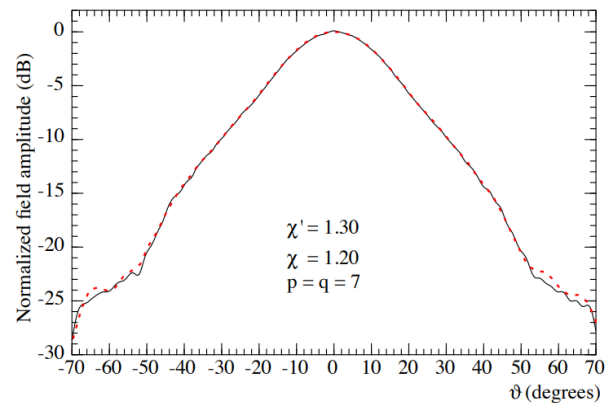


Fig. 4. H-plane pattern. — reconstructed from plane-rectangular NF data. - - - reconstructed from the non-redundant plane-polar NF samples with hardware co-rotation.

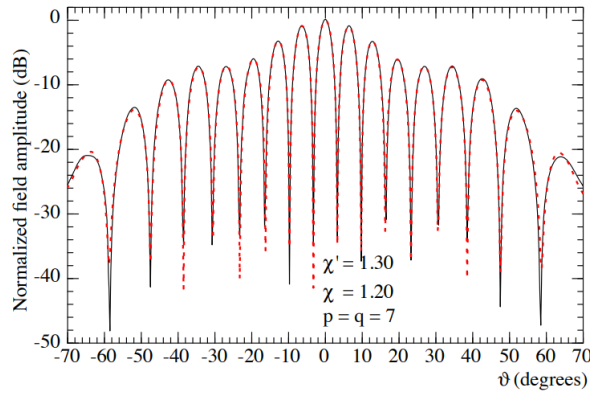


Fig. 5. E-plane pattern. — reconstructed from plane-rectangular NF data. - - - reconstructed from the non-redundant plane-polar NF samples with software co-rotation.

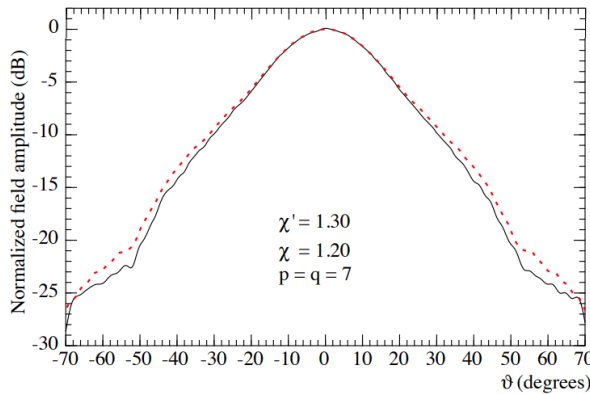


Fig. 6. H-plane pattern. — reconstructed from plane-rectangular NF data. - - - reconstructed from the non-redundant plane-polar NF samples with software co-rotation.

The amplitude and phase of  $V_\rho$  on the diameter at  $\varphi = 90^\circ$ , retrieved via the SVD procedure, are compared in Figs. 7 and 8 with the ones directly measured on the same line. The comparison between the recovered amplitude of  $V_\rho$  on the diameter at  $\varphi = 0^\circ$  and that directly measured is also reported in Fig. 9. As can be clearly observed, notwithstanding the imposed severe values of the positioning errors, all recoveries are very accurate except for the zones where the voltage level is very low.

To put in evidence only the error related to the retrieval of the uniform samples from the acquired non-uniform ones and not just that imputable to the software co-rotation, the overall efficacy of the SVD based technique is validated by comparing the FF patterns in the principal planes E and H (Figs. 10 and 11) recovered from the non-uniform NF data with the ones reconstructed from

the non-redundant, uniform, plane-polar NF samples with software co-rotation (reference). The reconstructed FF patterns obtained from the non-uniform plane-polar NF data without using the SVD technique are shown in the same figures for sake of comparison. These last reconstructions appear remarkably worsened with respect to the ones obtained when applying the SVD based procedure, thus further assessing its effectiveness for compensating known position errors. Since the considered set of non-uniform samples satisfies also the applicability conditions for the iterative procedure, this last has been applied too by obtaining quite analogous results, as can be seen from Figs. 12 and 13.

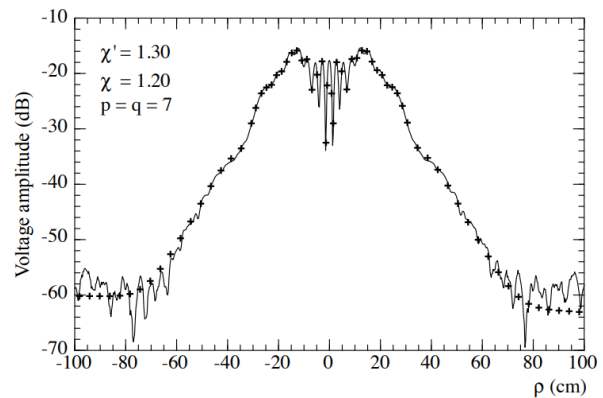


Fig. 7.  $V_\rho$  amplitude on the diameter at  $\varphi = 90^\circ$ . — measured. + + + retrieved from the non-uniform NF samples via the SVD procedure.

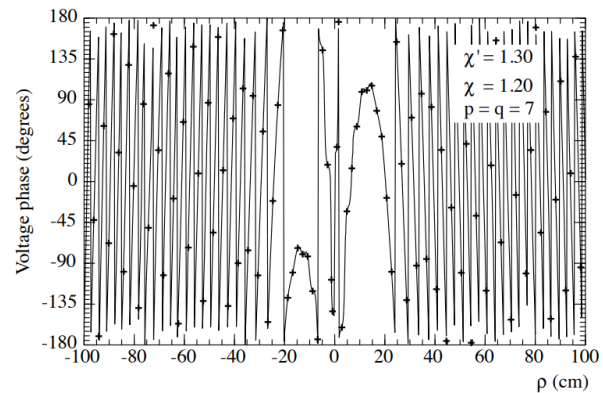


Fig. 8.  $V_\rho$  phase on the diameter at  $\varphi = 90^\circ$ . — measured. + + + retrieved from the non-uniform NF samples via the SVD procedure.

The second set of figures (from Fig. 14 to Fig. 18) refers to the case of non-uniform sampling points which do not lie on rings and, therefore, the iterative technique has been adopted. In this case, the not regularly spaced samples have been collected in such a way that the random shifts in  $\eta$  and  $\varphi$  between the positions of the non-uniform samples

and the related uniform ones are uniformly distributed in  $(-\Delta\eta/3, \Delta\eta/3)$  and  $(-\Delta\varphi_n/3, \Delta\varphi_n/3)$ . Figures 14 and 15 show the comparison between the amplitudes of  $V_\rho$  and  $V_\varphi$  on the diameter at  $\varphi = 30^\circ$  recovered from the non-uniform samples by applying the iterative procedure and the directly acquired ones on the line. The reconstruction of the phase of the most significant of them is shown in Fig. 16 for completeness. Also in such a case, the reconstructions are very accurate. It should be noticed that the above results have been got by using only 10 iterations, since, as shown in [25], such a number of iterations guarantees that the iterative scheme converges with very low errors. At last, the overall efficacy of the iterative technique for correcting known probe positioning errors is confirmed by the E-plane and H-plane pattern reconstructions reported in Figs. 17 and 18. As a matter of fact, the reconstructions obtained without using the iterative approach, reported in the same figures, appear severely compromised.

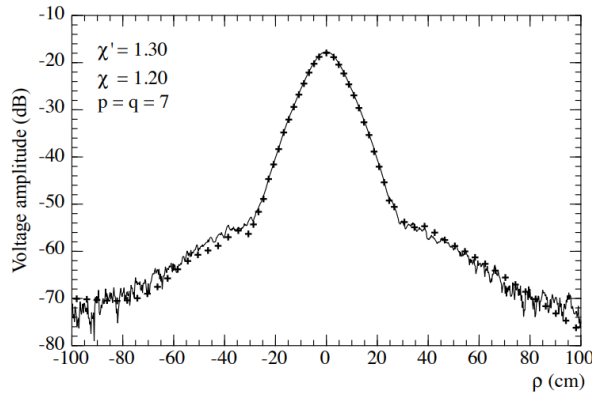


Fig. 9.  $V_\varphi$  amplitude on the diameter at  $\varphi = 0^\circ$ . — measured. ++++ retrieved from the non-uniform NF samples via the SVD procedure.

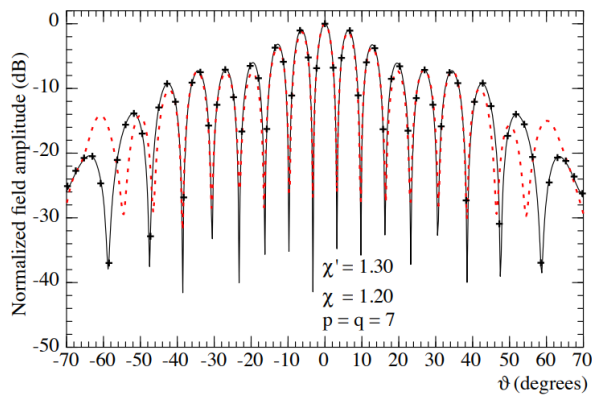


Fig. 10. E-plane pattern. — reference. ++++ recovered from the non-uniform NF samples via the SVD procedure. ---- recovered without using the SVD procedure.

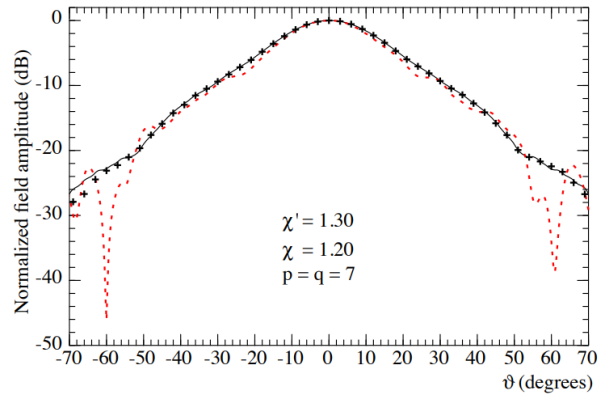


Fig. 11. H-plane pattern. — reference. ++++ recovered from the non-uniform NF samples via the SVD procedure. ---- recovered without using the SVD procedure.

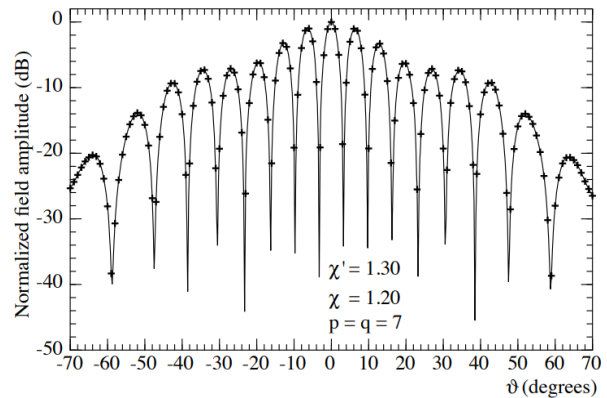


Fig. 12. E-plane pattern. — recovered from the non-uniform NF samples via the SVD procedure. ++++ recovered from the non-uniform NF samples via the iterative procedure.

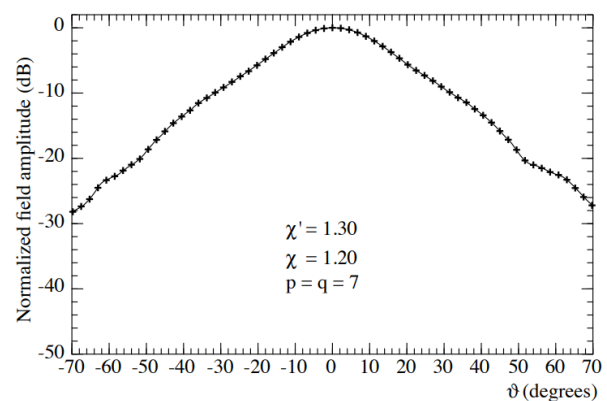


Fig. 13. H-plane pattern. — recovered from the non-uniform NF samples via the SVD procedure. ++++ recovered from the non-uniform NF samples via the iterative procedure.

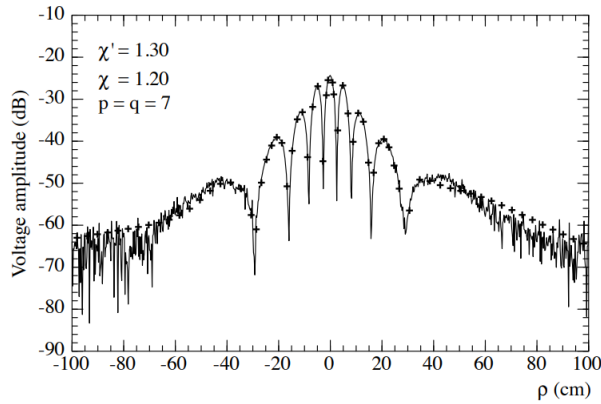


Fig. 14.  $V_\rho$  amplitude on the diameter at  $\varphi = 30^\circ$ . — measured. + + + + retrieved from the non-uniform NF samples via the iterative procedure.

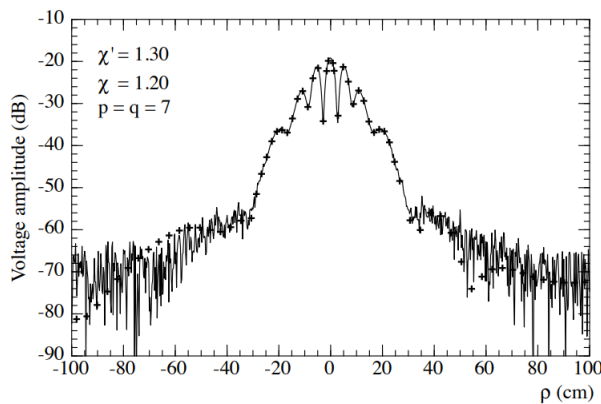


Fig. 15.  $V_\varphi$  amplitude on the diameter at  $\varphi = 30^\circ$ . — measured. + + + + retrieved from the non-uniform NF samples via the iterative procedure.

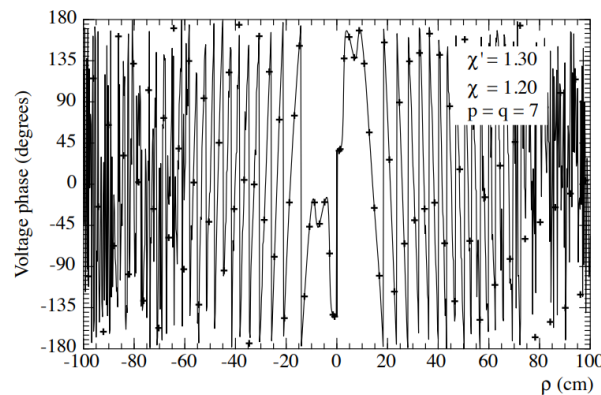


Fig. 16.  $V_\varphi$  phase on the diameter at  $\varphi = 30^\circ$ . — measured. + + + + retrieved from the non-uniform NF samples via the iterative procedure.

It is worthy to point out that the number of the collected

not regularly spaced plane-polar NF samples is 1476 in both the cases and, accordingly, remarkably less than (33 581) required by the plane-polar scanning techniques [8, 9] to cover the same measurement area.

Another set of experimental results, validating the effectiveness of the two developed techniques and relevant to a different antenna, can be found in [32].

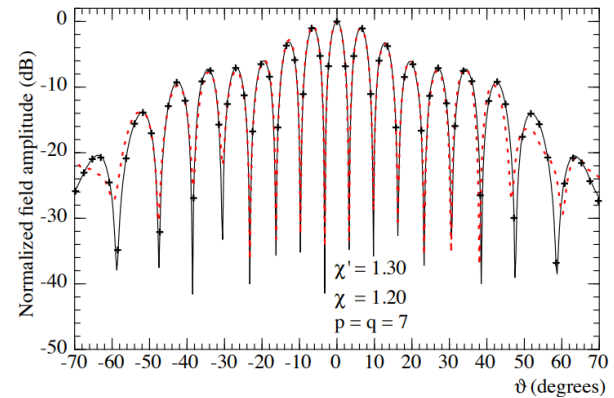


Fig. 17. E-plane pattern. — reference. + + + + recovered from the non-uniform NF samples via the iterative procedure. - - - - recovered without using the iterative procedure.

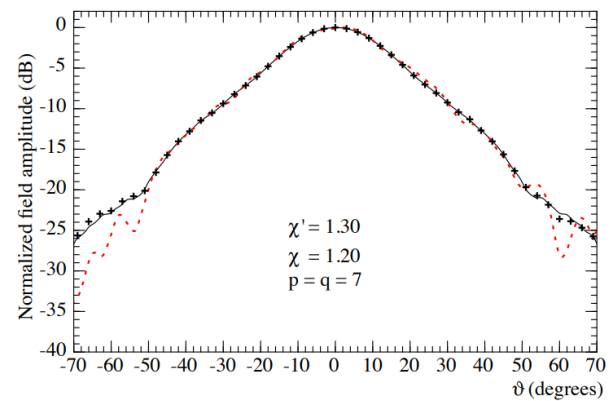


Fig. 18. H-plane pattern. — reference. + + + + recovered from the non-uniform NF samples via the iterative procedure. - - - - recovered without using the iterative procedure.

#### IV. CONCLUSION

In this paper, two effective procedures, which allow the correction of known positioning errors in the plane-polar NTF transformation based on the double bowl AUT model, have been proposed. The very good NF and FF reconstructions attained when applying them in presence of large and pessimistic positioning errors, as compared with the worsened ones obtained when these procedures are not employed, validate experimentally their

effectiveness.

## REFERENCES

- [1] A. D. Yaghjian, "An overview of near-field antenna measurements," *IEEE Trans. Antennas Prop.*, vol. AP-34, pp. 30-45, Jan. 1986.
- [2] E. S. Gillespie, Ed., "Special issue on near-field scanning techniques," *IEEE Trans. Antennas Prop.*, vol. 36, pp. 727-901, June 1988.
- [3] M. H. Francis and R. W. Wittmann, "Near-field scanning measurements: Theory and practice," in *Modern Antenna Handbook*, C.A. Balanis, Ed., chapter 19, John Wiley & Sons, Hoboken, NJ, USA, 2008.
- [4] M. H. Francis, Ed., *IEEE Recommended Practice for Near-Field Antenna Measurements*, IEEE Standard 1720-2012, 2012.
- [5] C. Gennarelli, A. Capozzoli, L. Foged, J. Fordham, and D. J. van Rensburg, Eds., "Recent advances in near-field to far-field transformation techniques," *Int. Jour. Antennas Prop.*, vol. 2012, ID 243203, 2012.
- [6] D. T. Paris, W. M. Leach, Jr., and E. B. Joy, "Basic theory of probe-compensated near-field measurements," *IEEE Trans. Antennas Prop.*, vol. AP-26, pp. 373-379, May 1978.
- [7] E. B. Joy, W. M. Leach, Jr., G. P. Rodrigue, and D. T. Paris, "Application of probe-compensated near-field measurements," *IEEE Trans. Antennas Prop.*, vol. AP-26, pp. 379-389, May 1978.
- [8] Y. Rahmat-Samii, V. Galindo Israel, and R. Mittra, "A plane-polar approach for far-field construction from near-field measurements," *IEEE Trans. Antennas Prop.*, vol. AP-28, pp. 216-230, Mar. 1980.
- [9] M. S. Gatti and Y. Rahmat-Samii, "FFT applications to plane-polar near-field antenna measurements," *IEEE Trans. Antennas Prop.*, vol. 36, pp. 781-791, June 1988.
- [10] A. D. Yaghjian, "Antenna coupling and near-field sampling in plane-polar coordinates," *IEEE Trans. Antennas Prop.*, vol. 40, pp. 304-312, Mar. 1992.
- [11] O. M. Bucci, C. Gennarelli, G. Riccio, and C. Savarese, "Near-field-far-field transformation from nonredundant plane-polar data: Effective modellings of the source," *IEE Proc. Microw., Antennas Prop.*, vol. 145, pp. 33-38, Feb. 1998.
- [12] O. M. Bucci, F. D'Agostino, C. Gennarelli, G. Riccio, and C. Savarese, "NF-FF transformation with plane-polar scanning: Ellipsoidal modelling of the antenna," *Automatika*, vol. 41, pp. 159-164, 2000.
- [13] F. D'Agostino, F. Ferrara, C. Gennarelli, R. Guerriero, and M. Migliozi, "Reconstruction of the antenna far-field pattern through a fast plane-polar scanning," *Appl. Comp. Electromagn. Soc. Jour.*, vol. 31, pp. 1362-1369, Dec. 2016.
- [14] F. D'Agostino, F. Ferrara, C. Gennarelli, R. Guerriero, and M. Migliozi, "Far-field pattern reconstruction from a nonredundant plane-polar near-field sampling arrangement: Experimental testing," *IEEE Antennas Wireless Prop. Lett.*, vol. 15, pp. 1345-1348, 2016.
- [15] O. M. Bucci, C. Gennarelli, and C. Savarese, "Representation of electromagnetic fields over arbitrary surfaces by a finite and nonredundant number of samples," *IEEE Trans. Antennas Prop.*, vol. 46, pp. 351-359, Mar. 1998.
- [16] A. Dutt and V. Rohklin, "Fast Fourier transforms for nonequispaced data," *Proc. SIAM Jour. Scie. Comput.*, vol. 14, pp. 1369-1393, Nov. 1993.
- [17] R. C. Wittmann, B. K. Alpert, and M. H. Francis, "Near-field antenna measurements using nonideal measurement locations," *IEEE Trans. Antennas Prop.*, vol. 46, pp. 716-722, May 1998.
- [18] R. C. Wittmann, B. K. Alpert, and M. H. Francis, "Near-field, spherical-scanning antenna measurements with nonideal probe locations," *IEEE Trans. Antennas Prop.*, vol. 52, pp. 2184-2186, Aug. 2004.
- [19] O. M. Bucci, C. Gennarelli, and C. Savarese, "Interpolation of electromagnetic radiated fields over a plane from nonuniform samples," *IEEE Trans. Antennas Prop.*, vol. 41, pp. 1501-1508, Nov. 1993.
- [20] F. D'Agostino, F. Ferrara, C. Gennarelli, R. Guerriero, and M. Migliozi, "Two effective approaches to correct the positioning errors in a spherical near-field-far-field transformation," *Electromagnetics*, vol. 36, pp. 78-93, 2016.
- [21] F. Ferrara, C. Gennarelli, G. Riccio, and C. Savarese, "Far field reconstruction from nonuniform plane-polar data: A SVD based approach," *Electromagnetics*, vol. 23, pp. 417-429, 2003.
- [22] F. Ferrara, C. Gennarelli, M. Iacone, G. Riccio, and C. Savarese, "NF-FF transformation with bi-polar scanning from nonuniformly spaced data," *Appl. Comp. Electromagn. Soc. Jour.*, vol. 20, pp. 35-42, Mar. 2005.
- [23] F. Ferrara, C. Gennarelli, G. Riccio, and C. Savarese, "NF-FF transformation with cylindrical scanning from nonuniformly distributed data," *Microw. Optical Technol. Lett.*, vol. 39, pp. 4-8, Oct. 2003.
- [24] F. D'Agostino, F. Ferrara, C. Gennarelli, R. Guerriero, and M. Migliozi, "On the compensation of probe positioning errors when using a nonredundant cylindrical NF-FF transformation," *Prog. Electromagn. Res. B*, vol. 20, pp. 321-335, 2010.
- [25] F. D'Agostino, F. Ferrara, C. Gennarelli, R. Guerriero, and M. Migliozi, "Two techniques for compensating the probe positioning errors in the spherical NF-FF transformation for elongated antennas," *The Open Electr. & Electron. Eng. Jour.*, vol. 5, pp. 29-36, 2011.
- [26] F. D'Agostino, F. Ferrara, C. Gennarelli, R. Guerriero, and M. Migliozi, "Probe position errors corrected near-field-far-field transformation with

spherical scanning,” *Appl. Comp. Electromagn. Soc. Jour.*, vol. 31, pp. 106-117, Feb. 2016.

- [27] F. D’Agostino, F. Ferrara, C. Gennarelli, R. Guerriero, and M. Migliozi, “Far-field pattern evaluation from data acquired on a spherical surface by an inaccurately positioned probe,” *IEEE Antennas Wireless Prop. Lett.*, vol. 15, pp. 402-405, 2016.
- [28] F. D’Agostino, F. Ferrara, C. Gennarelli, R. Guerriero, and M. Migliozi, “Two efficient procedures to correct the positioning errors in the plane-polar scanning,” *IET Microw., Antennas & Prop.*, vol. 10, no. 13, pp. 1453-1458, 2016.
- [29] O. M. Bucci, G. D’Elia, and M. D. Migliore, “Advanced field interpolation from plane-polar samples: Experimental verification,” *IEEE Trans. Antennas Prop.*, vol. 46, pp. 204-210, Feb. 1998.
- [30] F. D’Agostino, F. Ferrara, C. Gennarelli, R. Guerriero, S. McBride, and M. Migliozi, “Fast and accurate antenna pattern evaluation from near-field data acquired via planar spiral scanning,” *IEEE Trans. Antennas Prop.*, vol. 64, Aug. 2016.
- [31] A. D. Yaghjian, “Approximate formulas for the far field and gain of open-ended rectangular waveguide,” *IEEE Trans. Antennas Prop.*, vol. AP-32, pp. 378-384, Apr. 1984.
- [32] F. D’Agostino, F. Ferrara, C. Gennarelli, R. Guerriero, and M. Migliozi, “Far-field reconstruction from plane-polar near-field data affected by probe position errors,” in *Proc. of AMTA 2015*, Long Beach, CA, pp. 308-313, Oct. 2015.



**Francesco D’Agostino** was born near Salerno (Italy) in 1965. He received the Laurea degree in Electronic Engineering from the University of Salerno in 1994, where in 2001 he received the Ph.D. degree in Information Engineering. From 2002 to 2005 he was Assistant Professor at the Engineering Faculty of the University of Salerno where, in October 2005, he was appointed Associate Professor of Electromagnetics and joined the Department of Industrial Engineering, where he is currently working. His research activity includes application of sampling techniques to electromagnetics and to innovative NF–FF transformations, diffraction problems radar cross section evaluations, Electromagnetic Compatibility. In this area, D’Agostino has co-authored 4 books and about 220 scientific papers, published in peer-reviewed international journals and conference proceedings. He is a regular

Reviewer for several journals and conferences and has chaired some international events and conferences. D’Agostino is a Member of AMTA, EurAAP, and IEEE.



**Flaminio Ferrara** was born near Salerno, Italy, in 1972. He received the Laurea degree in Electronic Engineering from the University of Salerno in 1999. Since the same year, he has been with the Research Group in Applied Electromagnetics at the University of Salerno. He received the Ph.D. degree in Information Engineering at the same University, where he is presently an Assistant Professor of Electromagnetic Fields. His interests include: application of sampling techniques to the efficient reconstruction of electromagnetic fields and to NF–FF transformation techniques; monostatic radar cross section evaluations of corner reflectors. Ferrara is co-author of about 220 scientific papers, mainly in international journals and conference proceedings. He is Reviewer for several international journals and Member of the Editorial board of the International Journal of Antennas and Propagation. He is Member of the IEEE society.



**Claudio Gennarelli** was born in Avellino, Italy, in 1953. He received the Laurea degree (*summa cum laude*) in Electronic Engineering from the University of Naples, Italy, in 1978. From 1978 to 1983, he worked with the Research Group in Electromagnetics at the Electronic Engineering Department of the University “Federico II” of Naples. In 1983, he became Assistant Professor at the Istituto Universitario Navale (IUN), Naples. In 1987, he was appointed Associate Professor of Antennas, formerly at the Engineering Faculty of Ancona University and subsequently at the Engineering Faculty of Salerno University. In 1999, he has been appointed Full Professor at the same University. The main topics of his scientific activity are: reflector antennas analysis, antenna measurements, diffraction problems, radar cross section evaluations, scattering from surface impedances, application of sampling techniques to electromagnetics and to NF–FF transformations. Gennarelli is co-author of about 400 scientific papers, mainly in international journals and conference proceedings. In particular, he is co-author of four books on NF–FF transformation techniques. He is a Senior Member of the IEEE and Member of the Editorial board of the Open Electrical and Electronic Engineering Journal and of the International Journal of Antennas and Propagation.



**Rocco Guerriero** received the Laurea degree in Electronic Engineering and the Ph.D. degree in Information Engineering from the University of Salerno in 2003 and 2007, respectively. Since 2003, he has been with the Research Group in Applied Electromagnetics of University of Salerno, where he is currently an Assistant Professor of Electromagnetic Fields. His interests include: application of sampling techniques to the efficient reconstruction of electromagnetic fields and to near-field-far-field transformation techniques; antenna measurements; inversion of ill-posed electromagnetic problems; analysis of microstrip reflectarrays; diffraction problems. Guerriero is co-author of about 180 scientific papers, mainly in international journals and conference proceedings. He is Reviewer for several international journals and Member of the Editorial board of the International Journal of

Antennas and Propagation. Since 2015, he is Member IEEE.



**Massimo Migliozi** received the Laurea degree in Electronic Engineering from the University of Salerno, in 1999. He received the Ph.D. degree in Information Engineering at the same University, where at the present time he is a Research Fellow in Electromagnetic Fields. His scientific interests include: application of sampling techniques to the efficient reconstruction of electromagnetic fields and to NF-FF transformation techniques; antenna measurements; electromagnetic compatibility; antenna design; diffraction problems. Migliozi is co-author of over 130 scientific papers, mainly in international journals and conference proceedings. He is Reviewer for several international journals.